

Homodinuclear Iron Thiolate Nitrosyl Compounds

[(ON)Fe(S,S-C₆H₄)₂Fe(NO)₂][−] and [(ON)Fe(SO₂,S-C₆H₄)(S,S-C₆H₄)Fe(NO)₂][−] with {Fe(NO)}^{7−}{Fe(NO)₂}⁹ Electronic Coupling: New Members of a Class of Dinitrosyl Iron ComplexesHao-Wen Chen,^{†‡} Chin-Wei Lin,[†] Chiao-Chun Chen,[‡] Li-Bo Yang,[†] Ming-Hsi Chiang,[†] and Wen-Feng Liaw^{*†}

Departments of Chemistry, National Tsing Hua University, Hsinchu 30043, and National Changhua University of Education, Changhua, Taiwan

Received July 8, 2004

Reaction of Fe(CO)₂(NO)₂ and [(ON)Fe(S,S-C₆H₃R)₂][−] (R = H (**1**), CH₃ (**1-Me**))/[(ON)Fe(SO₂,S-C₆H₄)(S,S-C₆H₄)][−] (**4**) in THF afforded the diiron thiolate/sulfinate nitrosyl complexes [(ON)Fe(S,S-C₆H₃R)₂Fe(NO)₂][−] (R = H (**2**), CH₃ (**2-Me**)) and [(ON)Fe(S,SO₂-C₆H₄)(S,S-C₆H₄)Fe(NO)₂][−] (**3**), respectively. The average N–O bond lengths ([Fe(NO)₂] unit) of 1.167(3) and 1.162(4) Å in complexes **2** and **3** are consistent with the average N–O bond length of 1.165 Å observed in the other structurally characterized dinitrosyl iron complexes with an {Fe(NO)₂}⁹ core. The lower ν(¹⁵NO) value (1682 cm^{−1} (KBr)) of the [(¹⁵NO)FeS₄] fragment of [(¹⁵NO)Fe(S,S-C₆H₃CH₃)₂Fe(NO)₂][−] (**2-Me-¹⁵N**), compared to that of [(¹⁵NO)Fe(S,S-C₆H₃CH₃)₂][−] (**1-Me-¹⁵N**) (1727 cm^{−1} (KBr)), implicates the electron transfer from {Fe(NO)₂}¹⁰ Fe(CO)₂(NO)₂ to complex **1-Me/1** may occur in the process of formation of complex **2-Me/2**. Then, the electronic structures of the [Fe(NO)S₄] and [S₂Fe(NO)₂] cores of complexes **2**, **2-Me**, and **3** were best assigned according to the Feltham–Enemark notation as the {Fe(NO)}^{7−}{Fe(NO)₂}⁹ coupling (antiferromagnetic interaction with a *J* value of −182 cm^{−1} for complex **2**) to account for the absence of paramagnetism (SQUID) and the EPR signal. On the basis of Fe–N(O) and N–O bond distances, the dinitrosyliron {L₂Fe(NO)₂} derivatives having an Fe–N(O) distance of ~1.670 Å and a N–O distance of ~1.165 Å are best assigned as {Fe(NO)₂}⁹ electronic structures, whereas the Fe–N(O) distance of ~1.650 Å and N–O distance of ~1.190 Å probably imply an {Fe(NO)₂}¹⁰ electronic structure.

Introduction

Iron sulfur nitrosyl complexes, in particular the dinitrosyl-iron compounds (DNICs), have attracted considerable interest stimulated by their structures, functions, and biological activities; e.g. (i) the formation of protein-bound dinitrosyl-iron complexes was reported in the anaerobic reaction of high-potential iron protein with nitric oxide,^{1,2} (ii) DNICs have been suggested as storage and transporters of NO *in vivo* as well as intermediates of iron-catalyzed degradation

and formation of *S*-nitrosothiols,^{3,4} (iii) activation of SoxR protein, a redox-sensitive transcription activator, in *Escherichia coli* on exposure to macrophage-generated NO has been suggested to occur through nitrosylation of the [2Fe–2S] clusters to form protein-bound dinitrosyliron dithiol adducts,⁵ and (iv) DNICs have been identified as endogenous NO carriers.⁴

Existence of the paramagnetic {Fe(NO)₂}⁹ DNICs [(RS)₂-Fe(NO)₂][−] is generally characterized by an isotopic EPR

* To whom correspondence should be addressed. E-mail: wfliaw@mx.nthu.edu.tw.

[†] National Tsing Hua University.

[‡] National Changhua University of Education.

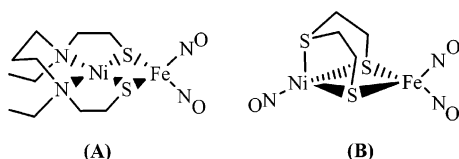
- (1) (a) Foster, M. W.; Cowan, J. A. *J. Am. Chem. Soc.* **1999**, *121*, 4093. (b) Morse, R. H.; Chan, S. I. *J. Biol. Chem.* **1980**, *255*, 7876. (c) Reginato, N.; McCrory, C. T. C.; Pervitsky, D.; Li, L. *J. Am. Chem. Soc.* **1999**, *121*, 10217. (2) (a) Cooper, C. E. *Biochim. Biophys. Acta* **1999**, *1411*, 290. (b) Vanin, A. F.; Stukan, R. A.; Manukhina, E. B. *Biochim. Biophys. Acta* **1996**, *1295*, 5.

- (3) (a) Vanin, A. F. *Biochemistry (Moscow)* **1998**, *63*, 782. (b) Wang, P. G.; Xian, M.; Tang, X.; Wu, X.; Wen, Z.; Cai, T.; Janczuk, A. J. *Chem. Rev.* **2002**, *102*, 1091. (c) Vanin, A. F. *Biochemistry (Moscow)* **1995**, *60*, 225. (d) Vanin, A. F.; Malenkova, I. V.; Serezhenkov, V. A. *Nitric Oxide Biol. Chem.* **1997**, *1*, 191.

- (4) Ford, P. C.; Bourassa, J.; Miranda, K.; Lee, B.; Lorkovic, I.; Boggs, S.; Kudo, S.; Laverman, L. *Coord. Chem. Rev.* **1998**, *171*, 185. (b) Ford, P. C.; Lorkovic, I. M. *Chem. Rev.* **2002**, *102*, 993. (c) Hayton, T. W.; Legzdins, P.; Sharp, W. B. *Chem. Rev.* **2002**, *102*, 935. (d) Wang, P. G.; Xian, M.; Tang, X.; Wu, X.; Wen, Z.; Cai, T.; Janczuk, A. J. *Chem. Rev.* **2002**, *102*, 1091.

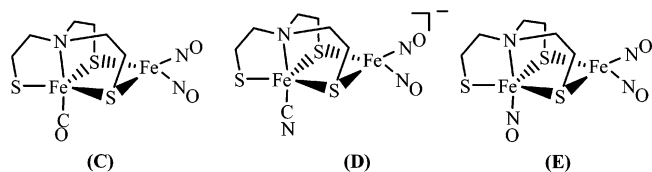
signal of $g = 2.03$.^{1–5} The oxidation level of the $\{\text{Fe}(\text{NO})_2\}$ unit in the paramagnetic $\{\text{Fe}(\text{NO})_2\}^9$ DNICs was verified, recently, in a study of the photochemistry of the dinitrosyliron complex $[\text{S}_5\text{Fe}(\text{NO})_2]^-$ leading to reversible formation of $[\text{S}_5\text{Fe}(\mu\text{-S})_2\text{FeS}_5]^{2-}$.⁶ DFT calculations, magnetic susceptibility measurements, EPR, and Fe K/L-edge XAS suggest the electronic structure of the $\{\text{Fe}(\text{NO})_2\}$ core of the complex $[\text{S}_5\text{Fe}(\text{NO})_2]^-$ is better described as $\{\text{Fe}^+(\bullet\text{NO})_2\}^9$ than as $\{\text{Fe}^-(\text{NO}^+)_2\}^9$. Rhombic EPR signals ($g_z = 2.0148$, $g_x = 2.0270$, and $g_y = 2.0485$) at 77 K confirmed the existence of the unpaired electron in $[\text{S}_5\text{Fe}(\text{NO})_2]^-$.⁶ In contrast, the neutral diamagnetic $\{\text{Fe}(\text{NO})_2\}^{10}$ DNICs $[\text{L}_2\text{Fe}(\text{NO})_2]$ are stabilized by neutral donor ligands such as $\text{L} = \text{PPh}_3$, CO , and N-containing ligands.⁴

Two heterobimetallic nickel–iron thiolate nitrosyl complexes containing a dinitrosyliron $\{\text{Fe}(\text{NO})_2\}^{10}/\{\text{Fe}(\text{NO})_2\}^9$ motif, $[\text{Ni}^{\text{II}}(\mu\text{-S}(\text{CH}_2)_2\text{N}(\text{Et})(\text{CH}_2)_3\text{N}(\text{Et})(\text{CH}_2)_2\text{S})\text{Fe}(\text{NO})_2]$ (**A**)⁷ and $[(\text{NO})\text{Ni}^0(\mu\text{-S}(\text{CH}_2)_2\text{S}(\text{CH}_2)_2\text{S})\text{Fe}(\text{NO})_2]$ (**B**),⁸ were



reported. Complexes **A** and **B** with Ni–Fe distances of 2.797(1) and 2.8001(6) Å, respectively, may be viewed as mononuclear $\text{Fe}(\text{NO})_2$ units with thiolate ligands modified by distal metal interactions. The distal Ni^{II} metal of complex **A** creates neutral sulfur donor sites and stabilizes the electron-rich or -reduced form $\{\text{Fe}(\text{NO})_2\}^{10}$, as does CO or PR_3 in the neutral DNICs $[\text{L}_2\text{Fe}(\text{NO})_2]$.⁹ The $\{\text{Ni}^0\text{NO}^+\}$ unit of complex **B** effectively generates a monoanionic dithiolate ligand donor set, which stabilizes the oxidized form $\{\text{Fe}(\text{NO})_2\}^9$. The different oxidation levels of the $\{\text{Fe}(\text{NO})_2\}^n$ unit in **A** and **B** also reflect the distinctly different hinge angles of the $\text{Ni}(\mu\text{-SR})_2\text{Fe}$ unit, 104.6° for complex **A** and 162.8° for complex **B**.^{7,8}

Additionally, diiron thiolate nitrosyl complexes $[\text{Fe}(\text{NO})_2\text{-}\{\text{Fe}(\text{NS}_3)(\text{CO})\}]$ (**C**), $[\text{Fe}(\text{NO})_2\{\text{Fe}(\text{NS}_3)(\text{CN})\}]^-$ (**D**), and $[\text{Fe}(\text{NO})_2\{\text{Fe}(\text{NS}_3)(\text{NO})\}]$ (**E**) ($\text{NS}_3 = [\text{N}(\text{CH}_2\text{CH}_2\text{S})_3]^{3-}$),



containing an $\text{Fe}(\text{NO})_2$ motif and a $\text{CO}/\text{CN}/\text{NO}$ ligand occupying the axial position of a trigonal bipyramidal Fe center, were also reported.¹⁰ It is proposed that the oxidation state of the iron of the $\text{Fe}(\text{NS}_3)$ motif in complexes **C**, **D**, and **E** is essentially unchanged upon its ligation to the $\text{Fe}(\text{NO})_2$ motif, and the oxidation state of the iron of the $\text{Fe}(\text{NS}_3)$ motif is $\text{Fe}(\text{II})$ in complexes **C** and **D** and $\text{Fe}(\text{III})$ in complex **E**.¹⁰ Here the metal nitrosyl unit is generally designated as $\{\text{M}(\text{NO})_x\}^n$ ($\text{M} = \text{transition metal}$).¹¹ This formalism $\{\text{M}(\text{NO})_x\}^n$ invokes the Enemark–Feltham notation, which stresses the well-known covalency and delocal-

ization in the electronically amorphous $\text{M}(\text{NO})_x$ unit,¹¹ without committing to a formal oxidation state on M , that is, assignments to $\text{M}^{\text{II}}(\text{NO}^-)_2$, $\text{M}^0(\bullet\text{NO})_2$, $\text{M}^{\text{II}}(\text{NO}^+)_2$, or some mixture thereof.

Despite a large number of mononuclear/tetranuclear iron thiolate nitrosyl complexes,^{10,12,13} examples of dinuclear iron thiolate complexes containing an $\{\text{Fe}(\text{NO})_2\}$ motif are limited.^{10,13} To gain understanding of the physical and chemical properties of dinitrosyliron complexes and mimic the metalloprotein-bound DNICs,^{1a} we have prepared complexes $[(\text{ON})\text{Fe}(\mu\text{-S},\text{S}-\text{C}_6\text{H}_3\text{R})_2\text{Fe}(\text{NO})_2]^-$ ($\text{R} = \text{H}$ (**2**), CH_3 (**2-Me**)) and $[(\text{ON})\text{Fe}(\text{S},\text{SO}_2-\text{C}_6\text{H}_4)(\text{S},\text{S}-\text{C}_6\text{H}_4)\text{Fe}(\text{NO})_2]^-$ (**3**). The isolated crystals of complexes **2**, **2-Me**, and **3** were characterized by IR, NMR, UV/vis, X-ray diffraction, EPR, and magnetic susceptibility measurements.

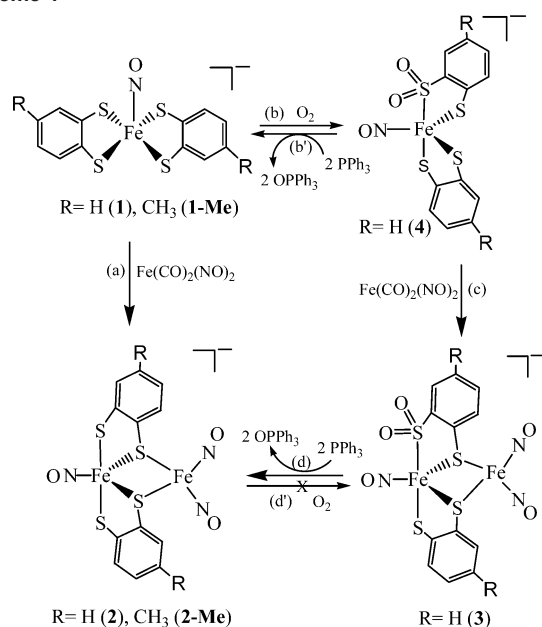
Results and Discussion

In contrast to NO binding to the $[(\text{C}_4\text{H}_8\text{O})\text{Fe}(\text{S},\text{S}-\text{C}_6\text{H}_4)_2]^-$, leading to the formation of $[\text{Fe}(\text{NO})(\text{S},\text{S}-\text{C}_6\text{H}_4)_2]^-$,¹⁴ the dark red-brown $[\text{Fe}(\text{NO})(\text{S},\text{S}-\text{C}_6\text{H}_3\text{R})_2]^-$ ($\text{R} = \text{H}$ (**1**), CH_3 (**1-Me**)) were prepared, alternatively, by reaction of 1,2-benzenedithiol (or toluene-3,4-dithiol, 0.8 mmol) and $[\text{Fe}(\text{CO})_5(\text{NO})]^-$ (0.4 mmol) in THF. Complexes **1** and **1-Me** are thermally stable and soluble in CH_2Cl_2 , THF, and CH_3CN . Diamagnetism of the magnetic measurements of complex **1/1-Me** is in accord with the ^1H NMR spectrum, which displays the expected signals (δ 6.87 (m), 7.65 (m) ppm (CDCl_3) for complex **1**) for the $[\text{S},\text{S}-\text{C}_6\text{H}_4]^{2-}$ ligands. The reversibility of the NO ligand lability of complex **1-Me** was demonstrated by exposing the THF solution of $[(^{15}\text{NO})\text{Fe}(\text{S},\text{S}-\text{C}_6\text{H}_3\text{CH}_3)_2]^-$ to a NO atmosphere. The IR ν_{NO} peak at 1727 cm^{-1} shifted to a single absorbance at 1763 cm^{-1} (KBr).

As shown in Scheme 1a, diiron thiolate nitrosyl complexes $[\text{PPN}][(\text{NO})\text{Fe}(\text{S},\text{S}-\text{C}_6\text{H}_3\text{R})_2\text{Fe}(\text{NO})_2]$ ($\text{R} = \text{H}$ (**2**), CH_3 (**2-Me**)) were synthesized in a single step by treating $\text{Fe}(\text{CO})_2(\text{NO})_2$ with complex **1/1-Me** in THF under a N_2 atmosphere at $10\text{ }^\circ\text{C}$. Complex **2**, soluble in THF, CH_2Cl_2 , and CH_3CN , was isolated as a dark green solid. The IR spectrum of complex **2** in the aprotic solvent THF reveals three $\nu(\text{NO})$ absorption bands at 1766 sh , 1746 vs , and 1719 s cm^{-1} .

- (5) Ding, H.; Demple, B. *Proc. Natl. Acad. Sci. U.S.A.* **2000**, *97*, 5146.
- (6) Tsai, M.-L.; Chen, C.-C.; Hsu, I.-J.; Ke, S.-C.; Hsieh, C.-H.; Chiang, K.-A.; Lee, G.-H.; Wang, Y.; Liaw, W.-F. *Inorg. Chem.* **2004**, *43*, 5159.
- (7) Osterloh, F.; Saak, W.; Haase, D.; Pohl, S. *Chem. Commun.* **1997**, 979.
- (8) Liaw, W.-F.; Chiang, C.-Y.; Lee, G.-H.; Peng, S.-M.; Lai, C.-H.; Darendsbourg, M. Y. *Inorg. Chem.* **2000**, *39*, 480.
- (9) (a) Hedberg, L.; Hedberg, K.; Satija, S. K.; Swanson, B. I. *Inorg. Chem.* **1985**, *24*, 2766. (b) Albano, V. G.; Araneo, A.; Bellon, P. L.; Ciani, G.; Manassero, M. J. *Organomet. Chem.* **1974**, *67*, 413.
- (10) Davies, S. C.; Evans, D. J.; Hughes, D. L.; Konkol, M.; Richards, R. L.; Sanders, J. R.; Sobota, P. J. *Chem. Soc., Dalton Trans.* **2002**, 2473.
- (11) Enemark, J. H.; Feltham, R. D. *Coord. Chem. Rev.* **1974**, *13*, 339.
- (12) (a) Chu, C. T.-W.; Dahl, L. F. *Inorg. Chem.* **1977**, *16*, 3245. (b) Chu, C. T.-W.; Lo, F. Y.-K.; Dahl, L. F. *J. Am. Chem. Soc.* **1982**, *104*, 3409. (c) Goh, C.; Holm, R. H. *Inorg. Chim. Acta* **1998**, *270*, 46. (d) Sung, S.-S.; Glidewell, C.; Butler, A. R.; Hoffmann, R. *Inorg. Chem.* **1985**, *24*, 3856.
- (13) Butler, A. R.; Glidewell, C.; Li, M.-H. *Adv. Inorg. Chem.* **1988**, *32*, 335.
- (14) Lee, C.-M.; Hsieh, C.-H.; Dutta, A.; Lee, G.-H.; Liaw, W.-F. *J. Am. Chem. Soc.* **2003**, *125*, 11492.

Scheme 1



Complex **2** exhibits a diagnostic ¹H NMR spectrum with resonances at δ 6.72–6.75 (m) and 7.44–7.62 (m) ppm (CDCl₃). On the basis of ¹H NMR, EPR, and magnetic measurements, complex **2** is characterized as a diamagnetic species.

Figure 1 displays a thermal ellipsoid plot of the anionic complex **2**, and selected bond distances and angles are given in Table 1. The geometry of Fe(1) of complex **2** is trigonal bipyramidal ([Fe(NO)(S)₄] core) with a NO ligand occupying the equatorial position (N(1)–Fe(1)–S(4) = 121.67(8)°, N(1)–Fe(1)–S(2) = 128.58(8)°, and S(4)–Fe(1)–S(2) = 109.75(3)°, while N(3)–Fe(2)–N(2) = 119.80(13)°, N(2)–Fe(2)–S(2) = 107.69(10)°, and S(4)–Fe(2)–S(2) = 106.06(3)° are consistent with the nearly regular tetrahedral coordination environment about Fe(2). In contrast to the distorted square pyramidal complex **1** with a S₄ base and an apical NO group,¹⁴ the geometry of Fe(1) in complex **2** is disturbed by the coordination of an additional [Fe(NO)₂] unit

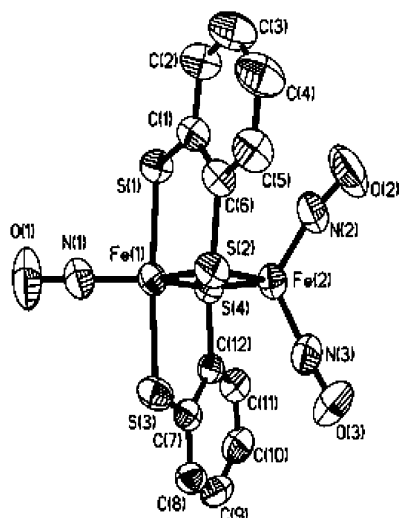


Figure 1. ORTEP drawing and labeling scheme of [(NO)Fe(S,S-C₆H₄)₂-Fe(NO)₂]⁻.

Table 1. Selected Bond Distances (Å) and Angles (deg) for Complexes **2** and **3**

Complex 2			
Fe(1)–N(1)	1.632(3)	Fe(1)–S(2)	2.2466(7)
Fe(1)–S(3)	2.3001(8)	Fe(1)–S(4)	2.2352(7)
Fe(1)–S(1)	2.2935(7)	Fe(1)–Fe(2)	2.6688(5)
Fe(2)–N(3)	1.660(3)	Fe(2)–N(2)	1.661(3)
Fe(2)–S(4)	2.2860(7)	Fe(2)–S(2)	2.3019(8)
N(1)–O(1)	1.167(3)	N(2)–O(2)	1.168(3)
N(3)–O(3)	1.167(3)		
N(1)–Fe(1)–S(4)	121.67(8)	S(4)–Fe(1)–S(2)	109.75(3)
S(4)–Fe(1)–S(1)	89.39(3)	S(4)–Fe(1)–S(3)	88.64(3)
S(1)–Fe(1)–S(3)	175.72(3)	N(1)–Fe(1)–Fe(2)	176.38(8)
N(2)–Fe(2)–N(3)	119.80(13)	N(2)–Fe(2)–S(4)	108.97(9)
N(2)–Fe(2)–S(2)	107.69(10)	N(1)–Fe(1)–S(2)	128.58(8)
S(4)–Fe(2)–S(2)	106.06(3)	O(1)–N(1)–Fe(1)	178.2(3)
O(3)–N(3)–Fe(2)	172.2(3)	O(2)–N(2)–Fe(2)	169.2(3)
Fe(1)–S(2)–Fe(2)	71.84(2)		
Complex 3			
Fe(1)–N(1)	1.641(3)	Fe(1)–S(2)	2.2272(9)
Fe(1)–S(3)	2.2929(11)	Fe(1)–S(4)	2.2318(9)
Fe(1)–S(1)	2.2630(10)	Fe(1)–Fe(2)	2.6482(7)
Fe(2)–N(3)	1.672(3)	Fe(2)–N(2)	1.671(3)
Fe(2)–S(4)	2.3005(10)	Fe(2)–S(2)	2.2728(10)
N(1)–O(1)	1.169(4)	N(2)–O(2)	1.160(4)
N(3)–O(3)	1.164(4)	S(1)–O(4)	1.459(3)
S(1)–O(5)	1.463(3)		
N(1)–Fe(1)–S(4)	130.49(11)	N(1)–Fe(1)–S(2)	119.30(11)
S(4)–Fe(1)–S(2)	110.20(4)	S(4)–Fe(1)–S(1)	89.97(3)
S(4)–Fe(1)–S(3)	88.80(3)	S(1)–Fe(1)–S(3)	177.81(4)
N(1)–Fe(1)–Fe(2)	174.05(11)	N(2)–Fe(2)–N(3)	121.12(16)
N(2)–Fe(2)–S(4)	108.41(12)	N(2)–Fe(2)–S(2)	103.28(11)
S(4)–Fe(2)–S(2)	106.19(4)	O(1)–N(1)–Fe(1)	178.4(3)
O(3)–N(3)–Fe(2)	169.7(4)	O(2)–N(2)–Fe(2)	173.4(3)
Fe(1)–S(2)–Fe(2)	72.09(3)		

to become trigonal bipyramidal. Such a geometrical change of the Fe(1) center from complex **1** to **2** may be accompanied by an electronic rearrangement resulting from a short Fe(1)···Fe(2) distance character (Fe(1)···Fe(2) distance of 2.6688(5) Å) and two bridging thiolate ligands.¹⁵ Ligand displacement resulting in the formation of complex **1** and {Fe(NO)₂}¹⁰ (PPh₃)₂Fe(NO)₂ was not observed when complex **2** was stirred with 2 equiv of PPh₃ in THF at room temperature for two weeks.⁹ In contrast, reaction of complex **2** and 2 equiv of [PPN][Sph] in THF solution at room temperature yielded the known {Fe(NO)₂}⁹ [(PhS)₂Fe(NO)₂]⁻⁸ and {Fe(NO)}⁷ [(NO)Fe(S,S-C₆H₄)₂]^{2-,16} which were characterized by IR, UV–vis, and X-ray single-crystal diffraction. On the basis of a recent study on the electronic structure of the {Fe(NO)₂}⁹ core of dinitrosyliron complex [S₃Fe(NO)₂]⁻⁶, and the reported qualitative MO energy level orderings for the five-coordinate {Fe(NO)}⁷ metal nitrosyl structure types (square pyramidal with bent apical NO, trigonal bipyramidal with linear equatorial NO, and trigonal bipyramidal with linear axial NO),¹⁵ the oxidation levels of the [S₂Fe(NO)₂] and [(NO)FeS₄] motifs of complex **2** may be assigned. For a five-coordinate metal nitrosyl complex, computational studies have suggested that a geometrical change from square pyramidal to trigonal bipyramidal with linear equatorial NO may occur upon changing from an {Fe(NO)}⁶ to an {Fe(NO)}⁷ electronic structure.¹⁵ Assignment to the oxidation

(15) Eisenberg, R.; Meyer, C. D. *Acc. Chem. Res.* **1975**, *8*, 26.

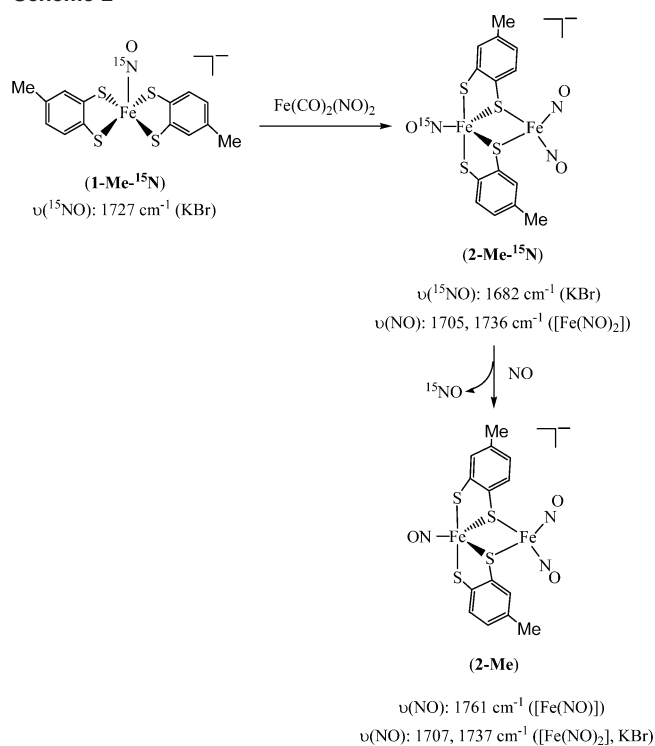
(16) Lee, C.-M.; Chen, C.-H.; Chen, H.-W.; Hsu, J.-L.; Lee, G.-H.; Liaw, W.-F. Submitted for publication.

levels of two Fe atoms of complex **2/2-Me** would, then, have to invoke electronic coupling of the $\{\text{Fe}(\text{NO})_2\}^9$ $[\text{S}_2\text{Fe}(\text{NO})_2]$ and the $\{\text{Fe}(\text{NO})\}^7$ $[(\text{NO})\text{FeS}_4]$ centers to account for the diamagnetism and the EPR silence in complex **2/2-Me**, although we cannot unambiguously rule out the possibility that the dimer formation (complexes **2** and **2-Me**) may simply involve partial charge delocalization around the diamond-shaped, planar $[\text{FeS}_2\text{Fe}]$ core in complex **2/2-Me**. The electronic configurations of the $\{\text{Fe}(\text{NO})\}^7$ and $\{\text{Fe}(\text{NO})_2\}^9$ centers are, therefore, best assigned as $\{\text{Fe}^+(\text{NO}^+)\}^7$ and $\{\text{Fe}^+(\text{NO})_2\}^9$ respectively. Both centers have $S = 1/2$ spins that magnetically couple to each other possibly via the pathway of direct d-d orbital overlap ($\text{Fe}\cdots\text{Fe} = 2.6688(5)$ Å) and the bridging sulfurs.¹⁷ The relatively strong magnetic interaction ($J = -182 \text{ cm}^{-1}$) leads to the ground state $S_T = 0$.¹⁷

Presumably, complex **2** was produced upon substitution of two carbonyls of $\text{Fe}(\text{CO})_2(\text{NO})_2$ by thiolate ligands of complex **1** accompanied by electron transfer from the $\{\text{Fe}(\text{NO})_2\}^{10}$ $[\text{Fe}(\text{NO})_2]$ unit of $[\text{Fe}(\text{CO})_2(\text{NO})_2]$ to $\{\text{Fe}(\text{NO})\}^6$ complex **1**. The proposed electron-donating/accepting process between $[\text{Fe}(2)(\text{NO})_2]$ and $[(\text{NO})\text{Fe}(1)\text{S}_4]$ units in the formation of complex **2** is also reflected in the ν_{NO} values. On treatment of $[(^{15}\text{NO})\text{Fe}(\text{S},\text{S}-\text{C}_6\text{H}_3\text{CH}_3)_2]^-$ (**1-Me-¹⁵N**) with 1 equiv of $\text{Fe}(\text{CO})_2(\text{NO})_2$ in THF, the reaction mixture led to the formation of the dinuclear $[(^{15}\text{NO})\text{Fe}(\text{S},\text{S}-\text{C}_6\text{H}_3\text{CH}_3)_2-\text{Fe}(\text{NO})_2]^-$ (**2-Me-¹⁵N**) showing three ν_{NO} infrared bands (1682 m, 1705 s, 1736 vs cm^{-1} (KBr)). Known to serve as a reporter of electron density at iron similarly to CO,^{18a} the lower $\nu(^{15}\text{NO})$ value (1682 cm^{-1} (KBr)) of the $[(^{15}\text{NO})\text{FeS}_4]$ fragment of **2-Me-¹⁵N**, compared to that of **1-Me-¹⁵N** (1727 cm^{-1} (KBr)), would then imply that the $[(^{15}\text{NO})\text{FeS}_4]$ unit of **2-Me-¹⁵N** is substantially reduced. That is, the $\{\text{Fe}(\text{NO})_2\}^{10}$ $[\text{Fe}(\text{NO})_2]$ unit of $\text{Fe}(\text{CO})_2(\text{NO})_2$ acts as a donor motif of -1 charge to **1-Me-¹⁵N** in the process of formation of complex **2-Me-¹⁵N**. When a THF solution of complex **2-Me-¹⁵N** is purged with NO, the IR ν_{NO} peaks (1682 m, 1705 s, 1736 vs cm^{-1}) shift to 1707 s, 1737 vs, and 1761 m cm^{-1} (KBr), consistent with the formation of complex **2-Me** (Scheme 2). The magnitude $\sim 55 \text{ cm}^{-1}$ of the isotopic shift ($\Delta\nu_{\text{NO}}$) is consistent with the calculated position, on the basis only of the difference in masses between ^{14}NO and ^{15}NO .

The Fe-N(1) distance of 1.599(2) Å in complex **1** is significantly shorter than those of $\{\text{Fe}(\text{NO})\}^7$ $[\text{Fe}(\text{NO})(\text{S}_2\text{CNMe}_2)_2]$ (Fe-N = 1.705(16) Å)^{18b} and $\{\text{Fe}(\text{NO})\}^8$ $[\text{Fe}(\text{NO})(\text{S}_2\text{C}_2\text{O}_2)_2]^{2-}$ (Fe-N = 1.690(2) Å).¹⁹ The shorter Fe-S bond distances of 2.226(11) Å (average) in complex **1**, compared with the reported Fe-S bond length of 2.294-(2) Å in $[\text{Fe}(\text{NO})(\text{S}_2\text{CNMe}_2)_2]$,^{18b} are attributed to the strong π -donating ability of the bidentate $[\text{S},\text{S}-\text{C}_6\text{H}_4]^{2-}$ ligands.²⁰

Scheme 2



Comparable to the shorter Fe-S (average 2.226(1) Å) and Fe-N(O) (1.599(2) Å) bond distances of complex **1**, the Fe-(1)-S (average 2.2689(8) Å) and Fe(1)-N(1) (1.632(3) Å) bond distances of complex **2** are disturbed by the coordination of an additional $[\text{Fe}(\text{NO})_2]$ unit. The Fe(1)-S_{bridging} bond length (average 2.2409(7) Å, Fe(1)-S(2) = 2.2466(7) Å and Fe(1)-S(4) = 2.2352(7) Å) is shorter than that of Fe(1)-S_{terminal} (average 2.2968(8) Å, Fe(1)-S(3) = 2.3001(8) Å and Fe(1)-S(1) = 2.2935(7) Å). The average Fe(2)-NO bond distance ($[\text{Fe}(\text{NO})_2]$ unit) of 1.661(3) Å (Fe(2)-N(3) = 1.660(3) Å and Fe(2)-N(2) = 1.661(3) Å) in complex **2** is within the ranges observed for other structurally characterized $\{\text{Fe}(\text{NO})_2\}^9$ complexes **B** (average Fe-N(O) = 1.672-(3) Å),⁷ $[(\text{NO})_2\text{Fe}(\text{SePh})_2]^-$ (average Fe-N(O) = 1.669(4) Å),⁸ and $[(\text{NO})_2\text{FeS}_5]^-$ (average Fe-N(O) = 1.678(3) Å),⁶ but significantly longer than the Fe-N(O) bond distances of 1.652(3) and 1.650(7) Å found in $\{\text{Fe}(\text{NO})_2\}^{10}$ complexes **A** and $(\text{PPh}_3)_2\text{Fe}(\text{NO})_2$, respectively.^{7,9} The Fe(1)-N(1) bond length of 1.632(3) Å in complex **2** is shorter than the Fe-NO bond distance (1.670(4) Å) found in $[(\text{NO})\text{Fe}(\text{TC}-5,5)]$.²¹

The ligand-modified analogue $[(\text{ON})\text{Fe}(\text{S},\text{SO}_2-\text{C}_6\text{H}_4)(\text{S},\text{S}-\text{C}_6\text{H}_4)]^-$ (**4**) is also expected to promote the formation of the diiron sulfinate nitrosyl complex (Scheme 1b). To corroborate this interpretation, we treated a THF solution of complex **4** with 1 equiv of $\text{Fe}(\text{CO})_2(\text{NO})_2$ at 10 °C (Scheme 1c).¹⁴ The IR ν_{NO} stretching frequencies (1726 s, 1762 s, 1783 m cm^{-1} (KBr)), UV-vis data, and X-ray structural study are consistent with the formation of $[(\text{ON})\text{Fe}(\text{S},\text{SO}_2-\text{C}_6\text{H}_4)(\text{S},\text{S}-\text{C}_6\text{H}_4)\text{Fe}(\text{NO})_2]^-$ (**3**). The higher ν_{NO} values of **3** versus **2** would then imply that the S-bonded monosulfinate substantially “neutralizes” the thiolate negative charge of

- (17) (a) Feig, A. L.; Bautista, M. T.; Lippard, S. T. *Inorg. Chem.* **1996**, *35*, 6892. (b) Kahn, O. *Molecular Magnetism*; VCH: New York, 1993.
- (18) (a) Horrocks, W. D.; Taylor, R. C. *Inorg. Chem.* **1963**, *2*, 723. (b) Davies, G. R.; Mais, R. H. B.; Owston, P. G. *Chem. Commun.* **1968**, 81.
- (19) Qian, L.; Singh, P.; Ro, H.; Hatfield, W. E. *Inorg. Chem.* **1990**, *29*, 761.
- (20) (a) Liaw, W.-F.; Lee, N.-H.; Chen, C.-H.; Lee, C.-M.; Lee, G.-H.; Peng, S.-M. *J. Am. Chem. Soc.* **2000**, *122*, 488. (b) Liaw, W.-F.; Hsieh, C.-K.; Lin, G.-Y.; Lee, G.-H. *Inorg. Chem.* **2001**, *40*, 3468.

- (21) Franz, K. J.; Lippard, S. J. *J. Am. Chem. Soc.* **1999**, *121*, 10504.

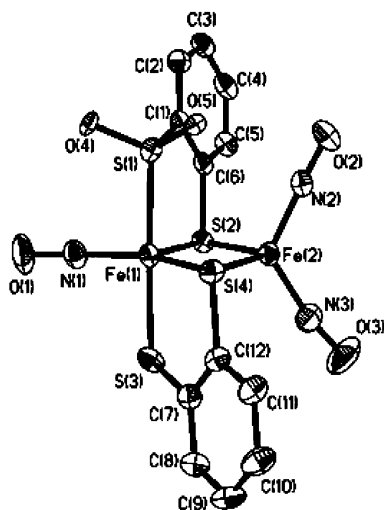


Figure 2. ORTEP drawing and labeling scheme of $[(\text{ON})\text{Fe}(\text{S},\text{SO}_2\text{-C}_6\text{H}_4)\text{-(S,S-C}_6\text{H}_4)\text{Fe}(\text{NO})_2]^-$.

complex **4**, and donates slightly less electron density to the $\{\text{Fe}(\text{NO})_2\}^9$ unit as compared to the two dithiolate donors of complex **2**. The ^1H NMR spectrum of complex **3** shows the expected signals for the 1,2-benzenedithiolate and -sulfinate groups involved and displays characteristics of diamagnetic species. As observed in complex **2**, the EPR and magnetic measurements of complex **3** also suggest the diamagnetism. Instead of formation of complex **4** and $\{\text{Fe}(\text{NO})_2\}^{10}$ $(\text{PPh}_3)_2\text{Fe}(\text{NO})_2$,⁹ the S-bonded monosulfinate complex **3** undergoes oxygen-transfer reaction in THF solution with 2 equiv of PPh_3 (expected to be an O atom abstracting agent) over the course of 90 min at 50 °C to yield complex **2** and triphenylphosphine oxide identified by ^{31}P NMR spectroscopy (Scheme 1d).²² This study also shows that complex **2** does not initiate O_2 activation to yield iron sulfinate complex **3** identified by IR spectra; complexes **1** and **4** and an insoluble solid were isolated instead.

The structure of complex **3** is presented in Figure 2. Analysis of the bond angles of complex **3** reveals that Fe(1) is best described as existing in a distorted trigonal bipyramidal coordination environment with NO and sulfinate groups occupying equatorial and axial positions, respectively. Distorted tetrahedral geometry is adopted in Fe(2). Consistent with other published transition-metal sulfinate complexes,²³ the S–O bond lengths average ca. 1.461(3) Å. The relief of the antibonding character from the Fe $d\pi/\text{S } p\pi$ overlap overwhelming the S-donating ability from thiolate to sulfinate may rationalize the observed shortening ($\Delta(\text{Fe}–\text{S}) = 0.03$ Å) of the Fe–S(O_2) bond length in complex **3**.²³ Presumably, the change in Fe(1)–Fe(2) distance (2.6625(2) Å for **2** and 2.6482(7) Å for **3**) is undoubtedly caused by electronic perturbations from the sulfur oxygenation. The shorter Fe(1)–Fe(2) distance of 2.6482(7) Å in complex **3** further implies an electronic interaction between the two metal centers, and an assignment of $\{\text{Fe}(\text{NO})\}^7\text{–}\{\text{Fe}(\text{NO})_2\}^9$

coupling would be realistic. The average N–O bond lengths ($[\text{Fe}(\text{NO})_2]$ unit) of 1.167(3) and 1.162(4) Å in complexes **2** and **3**, respectively, are comparable to those of the other structurally characterized $\{\text{Fe}(\text{NO})_2\}^9$ complexes **B** (average N–O = 1.161(3) Å),⁷ $[(\text{NO})_2\text{Fe}(\text{SePh})_2]^-$ (average N–O = 1.162(5) Å),⁸ and $[(\text{NO})_2\text{FeS}_5]^-$ (average N–O = 1.177(3) Å),⁶ but significantly shorter than the N–O bond lengths of 1.190(7) and 1.190(10) Å (average) observed in $\{\text{Fe}(\text{NO})_2\}^{10}$ complexes **A** and $(\text{PPh}_3)_2\text{Fe}(\text{NO})_2$, respectively.^{7,9} Consistent with the observation in complex **B**, the hinge angle of the $\text{Fe}(\mu\text{-SR})_2\text{Fe}$ unit, 178.9° for **2** and 178° for **3**, also supports a $[(\text{NO})\text{FeS}_4]^-/[(\text{NO})\text{FeS}_3(\text{SO}_2)]^-$ moiety bound by an $\{\text{Fe}(\text{NO})_2\}^9$ unit.⁸

Conclusion and Comments

Studies on the dinuclear iron thiolate nitrosyl complexes **2/2-Me** and **3** have led to the following results.

(1) Dinuclear iron thiolate/sulfinate nitrosyl complexes **2/2-Me** and **3** stabilized by $\{\text{Fe}(1)(\text{NO})\}^7\text{–}\{\text{Fe}(2)(\text{NO})_2\}^9$ coupling were synthesized and characterized by IR, UV–vis, ^1H NMR, and X-ray single-crystal diffraction. The magnetic coupling between the $\{\text{Fe}(\text{NO})\}^7$ and $\{\text{Fe}(\text{NO})_2\}^9$ centers (J value of -182 cm^{-1} in complex **2**) is responsible for the absence of paramagnetism (SQUID) and the EPR signal in complexes **2/2-Me** and **3**.

(2) The roughly planar structure in the $[\text{Fe}_2\text{S}_2\text{Fe}]$ core of complexes **2** and **3** (hinge angles 178.9° and 178°, respectively) also supports that complex **2/3** is best described as a $[(\text{NO})\text{FeS}_4]/[(\text{NO})\text{FeS}_3(\text{SO}_2)]$ moiety bound by an interacting $\{\text{Fe}(\text{NO})_2\}^9$ unit, respectively.

(3) In contrast to the distorted square pyramidal complex **1/1-Me** with a S_4 base and an apical NO group,¹⁴ the geometry of Fe(1) in complex **2** becomes trigonal bipyramidal upon complex **1** being coordinated by an additional $[\text{Fe}(\text{NO})_2]$ unit.

(4) For the formation mechanism of complex **2/3**, the isotopic experiments imply that the $\{\text{Fe}(\text{NO})_2\}^{10}$ $[\text{Fe}(\text{NO})_2]$ unit of $\text{Fe}(\text{CO})_2(\text{NO})_2$ acts as a donor motif of -1 charge to complex **1/4** to yield the stable diiron thiolate/sulfinate nitrosyl complex **2/3** containing an $\{\text{Fe}(\text{NO})_2\}^9$ motif, respectively.

(5) From the viewpoint of the Fe–N(O) and N–O bond distances, the dinitrosyliron $\{\text{Fe}(\text{NO})_2\}$ derivatives having an Fe–N(O) distance of ~ 1.670 Å and a N–O distance of ~ 1.165 Å are best assigned as $\{\text{Fe}(\text{NO})_2\}^9$ electronic structures. The much shorter Fe–N(O) distance of ~ 1.650 Å and longer N–O distance of ~ 1.190 Å probably imply an $\{\text{Fe}(\text{NO})_2\}^{10}$ electronic structure.

Isolation and characterization of the dinuclear iron thiolate nitrosyl complexes **2/2-Me** and **3** containing a dinitrosyl iron motif may be useful for taking into consideration the formation/existence of the metalloprotein-bound dinitrosyl-iron complexes in the anaerobic reaction of iron–sulfur protein and nitric oxide.^{1–5} Also, the findings in this study imply that the dinitrosyl nonheme iron complexes may exist after biosynthetic evolution of NO *in vitro* and from the

(22) Buonomo, R. M.; Font, I.; Maguire, M. J.; Reibenspies, J. H.; Tuntulani, T.; Darensbourg, M. Y. *J. Am. Chem. Soc.* **1995**, *117*, 963–973.

(23) Grapperhaus, C. A.; Darensbourg, M. Y. *Acc. Chem. Res.* **1998**, *31*, 451–459.

addition of NO to iron-centered proteins, even without the characteristic isotropic EPR signal of $g = 2.03$.²⁴

Experimental Section

Manipulations, reactions, and transfers of samples were conducted under nitrogen according to standard Schlenk techniques or in a glovebox (argon gas). Solvents were distilled under nitrogen from appropriate drying agents (hexane and tetrahydrofuran (THF) from sodium/benzophenone, diethyl ether and methylene chloride from CaH₂, and acetonitrile from CaH₂-P₂O₅) and stored in dried, N₂-filled flasks over 4 Å molecular sieves. Nitrogen was purged through these solvents before use. Solvent was transferred to a reaction vessel via a stainless steel cannula under a positive pressure of N₂. The reagents iron pentacarbonyl, sodium nitrite, toluene-3,4-dithiol, and 1,2-benzenedithiol (Lancaster/Aldrich) were used as received. Compounds [PPN][Fe(CO)₃(NO)], Fe(CO)₂(NO)₂, and [PPN][(ON)Fe(S,S-C₆H₄)₂] were synthesized and characterized by published procedures.^{9,14} Infrared spectra of the $\nu_{\text{NO}}/\nu_{\text{CO}}$ stretching frequencies were recorded on a Perkin-Elmer model Spectrum One B spectrometer with sealed solution cells (0.1 mm) and KBr windows. ¹H NMR spectra were recorded on a Varian Unity-500 spectrometer. GBC Cintra 10e spectrophotometers were used to record the UV-vis spectra of each complex. Analyses of carbon, hydrogen, and nitrogen were obtained with a CHN analyzer (Heraeus).

Preparation of [PPN][(ON)Fe(S,S-C₆H₃CH₃)₂] (1-Me). Toluene-3,4-dithiol (0.8 mmol, 100 μ L) was added to a THF solution (5 mL) of [PPN][Fe(CO)₃(NO)] (0.4 mmol, 0.283 g), and the resulting solution was stirred overnight at room temperature in contact with air. The reaction was monitored with FTIR. The IR spectrum (IR (THF): 1785 s (ν_{NO}) cm⁻¹) was assigned to the formation of **1-Me**.¹⁴ The solution was then filtered through Celite, and hexane (15 mL) was added to precipitate the dark red-brown solid **1-Me** (yield 0.3356 g, 90%). Diffusion of hexane into a THF solution of complex **1-Me** at -15 °C for 2 weeks gave dark red-brown crystals suitable for X-ray crystallography. IR (ν_{NO}): 1785 s (THF); 1763 s (KBr) cm⁻¹. ¹H NMR (CDCl₃): δ 2.20 (s) (CH₃); 6.693 (d), 7.51–7.55 (m) (C₆H₃) ppm. Absorption spectrum (THF) [λ_{max} , nm (ϵ , M⁻¹ cm⁻¹): 321 (37700), 500 (4200)]. Anal. Calcd for C₅₀H₄₂OFeN₂S₄P₂: C, 64.37; H, 4.54; N, 3.00. Found: C, 64.25; H, 4.19; N, 3.51.

Preparation of [PPN][(ON)Fe(μ -S,S-C₆H₃R)₂Fe(NO)₂] (R = H (2), CH₃ (2-Me)). Compound **1** (0.5 mmol, 0.452 g) was dissolved in 2 mL of dry THF, and 5 mL of a THF solution of Fe(CO)₂(NO)₂ (0.5 mmol) prepared freshly (obtained from reaction of [NO][PF₆] and [PPN][Fe(CO)₃(NO)] in THF in a 1:1 ratio)⁹ was added to it by cannula under a positive pressure of N₂. The reaction mixture was stirred at 10 °C for 1 h. The solution was then filtered through Celite, and hexane was added to precipitate a green solid. The solid was washed twice with THF-hexane and dried under vacuum. The yield of complex **2** was 0.418 g (80%). X-ray-quality crystals were obtained by diffusion of hexane into a saturated THF solution of complex **2** at -15 °C. The following are data for **2**. IR (ν_{NO}): 1766 sh, 1746 vs, 1719 s (THF); 1768 sh, 1748 s, 1720 s (CH₂Cl₂); 1759 m, 1735 vs, 1715 s (KBr) cm⁻¹. ¹H NMR (CDCl₃): δ 6.72–6.75 (m), 7.44–7.62 (m) ppm (C₆H₄). Absorption spectrum (CH₂Cl₂) [λ_{max} , nm (ϵ , M⁻¹ cm⁻¹): 313 (46619), 363 (15936), 417 (7557), 623 (3059), 790 (1367)]. Anal. Calcd for C₄₈H₃₈O₃N₄P₂S₄Fe₂: C, 56.48; H, 3.75; N, 5.49. Found: C, 56.29; H, 3.66; N, 5.55. The following are data for **2-Me**. IR (ν_{NO}): 1764 sh, 1745 vs, 1717 s (THF); 1761 m, 1737 vs, 1707 s (KBr) cm⁻¹.

Table 2. Crystallographic Data of Complexes **2** and **3**

	2	3
empirical formula	C ₄₈ H ₃₈ Fe ₂ N ₄ O ₃ P ₂ S ₄	C ₄₈ H ₃₈ Fe ₂ N ₄ O ₃ P ₂ S ₄
fw	1020.70	1052.70
cryst syst	monoclinic	monoclinic
space group	<i>P</i> 2 ₁ / <i>n</i>	<i>P</i> 2 ₁ / <i>n</i>
λ , Å (Mo K α)	0.71073	0.71073
<i>a</i> , Å	10.3579(4)	10.2033(4)
<i>b</i> , Å	24.8932(11)	25.0154(9)
<i>c</i> , Å	18.2655(8)	18.2842(6)
α , deg	90	90
β , deg	93.8840(10)	91.941(1)
γ , deg	90	90
<i>V</i> , Å ³	4698.8(3)	4664.2(3)
<i>Z</i>	4	4
<i>d</i> _{calcd} , g cm ⁻³	1.443	1.499
μ , mm ⁻¹	0.909	0.921
<i>T</i> , K	150(2)	150(1)
<i>R</i>	0.0369 ^a	0.0615 ^a
<i>R</i> _w	0.1015 ^b	0.1334 ^b
GOF	0.749	1.276

$$^a R = \sum|(F_o - F_c)|/\sum F_o, ^b R_w = \{\sum w(F_o^2 - F_c^2)^2/\sum w(F_o^2)\}^{1/2}$$

¹H NMR (CDCl₃): δ 2.088 (s), 2.117 (s) (CH₃); 6.518–6.543 (m), 7.579–7.635 (m) (C₆H₃) ppm. Absorption spectrum (THF) [λ_{max} , nm (ϵ , M⁻¹ cm⁻¹): 370 (10465), 427 (5266), 590 (2038), 650 (2129), 793 (1160)]. Anal. Calcd for C₅₀H₄₂O₃N₄P₂S₄Fe₂: C, 57.26; H, 4.04; N, 5.34. Found: C, 57.66; H, 4.38; N, 4.85.

The analogous [¹⁵N]nitrosyl complexes **1-Me-¹⁵N** and **2-Me-¹⁵N** were prepared as above using enriched [PPN][¹⁵NO₂] to prepare the starting material [PPN][Fe(CO)₃(¹⁵NO)].

Preparation of [PPN][(ON)Fe(S,SO₂-C₆H₄)(S,S-C₆H₄)Fe(NO)₂] (3). Compound [PPN][(ON)Fe(S,SO₂-C₆H₄)(S,S-C₆H₄)] (0.2 mmol, 0.187 g) was dissolved in 2 mL of dry THF in a 25 mL Schlenk tube, 5 mL of a THF solution of Fe(CO)₂(NO)₂ (0.2 mmol) prepared freshly was added to it by cannula under a positive pressure of N₂, and the resulting solution was stirred at 10 °C for 1 h.¹⁴ The solution was then filtered through Celite, and hexane was added to precipitate a green solid. The solid was washed twice with THF-hexane, and the yield of **3** was 0.150 g (71%). X-ray-quality crystals were obtained by diffusion of hexane-diethyl ether into a saturated CH₂Cl₂ solution of complex **3** at -15 °C. IR: 1783 m, 1762 s, 1726 s (ν_{NO}); 1192 m, 1055 m (ν_{SO}) (KBr); 1790 sh, 1771 s, 1733 m (ν_{NO}) (CH₂Cl₂); 1787 sh, 1768 s, 1733 m (ν_{NO}) (THF) cm⁻¹. ¹H NMR (CD₂Cl₂): δ 6.832 (t), 7.174 (t), 7.252 (t), 7.260 (d), 7.332 (d), 7.722 (d), 7.772 (d) ppm (C₆H₄). Absorption spectrum (CH₂Cl₂) [λ_{max} , nm (ϵ , M⁻¹ cm⁻¹): 305 (33836), 363 (14272), 595 (2113), 717 (1468)]. Anal. Calcd for C₄₈H₃₈O₅N₄P₂S₄Fe₂: C, 54.765; H, 3.64; N, 5.32. Found: C, 54.96; H, 3.49; N, 5.28.

Magnetic Measurements. The magnetic data were recorded on a SQUID magnetometer (MPMS5, Quantum Design) under a 1 T external magnetic field in the temperature range of 2–300 K. The magnetic susceptibility data were corrected with temperature-independent paramagnetism (TIP; 2×10^{-4} cm³ mol⁻¹) and the ligand diamagnetism by the tabulated Pascal constants. The equation for one *J* spin-coupled system is derived from the Hamiltonian and Van Vleck's equation. The magnetic coupling constant *J* of **2** is obtained from the least-squares fit of the magnetic susceptibility data.

Crystallography. Crystallographic data of complexes **2** and **3** are summarized in Table 2. The crystals of **2** and **3** chosen for X-ray single-crystal diffraction studies were measured 0.50 \times 0.50 \times 0.30 and 0.30 \times 0.25 \times 0.25 mm, respectively. Each crystal was mounted on a glass fiber and quickly coated in epoxy resin. Unit cell parameters were obtained by least-squares refinement. Diffraction measurements for complexes **2** and **3** were carried out at 150(1) K on a SMART CCD diffractometer with graphite-

(24) Reginato, N.; McCrory, C. T. C.; Pervitsky, D.; Li, L. *J. Am. Chem. Soc.* **1999**, *121*, 10217.

monochromated Mo K α radiation ($\lambda = 0.7107 \text{ \AA}$) and θ between 1.38° and 28.31° for complex **2** and between 1.38° and 27.50° for complex **3**. Least-squares refinement of the positional and anisotropic thermal parameters of all non-hydrogen atoms and fixed hydrogen atoms was based on F^2 . A SADABS²⁵ absorption correction was made. The SHELXTL²⁶ structure refinement program was employed. In the case of complex **3**, the S(1)O₂ group (shown in Figure 2) is found at disordered positions (O(4)O(5): O(4')O(5') = 1/2:1/2) and was refined by partial occupancies.

(25) Sheldrick, G. M. *SADABS, Siemens Area Detector Absorption Correction Program*; University of Göttingen: Göttingen, Germany, 1996.

(26) Sheldrick, G. M. *SHELXTL, Program for Crystal Structure Determination*; Siemens Analytical X-ray Instruments Inc.: Madison, WI, 1994.

Acknowledgment. We gratefully acknowledge financial support from the National Science Council (Taiwan). We appreciate the assistance of Fen-Ling Liao (National Tsing Hua University, Taiwan).

Supporting Information Available: X-ray crystallographic files in CIF format for the structure determinations of [PPN][Fe(NO)(S,S-C₆H₄)₂Fe(NO)₂] and [PPN][Fe(ON)(S,SO₂-C₆H₄)(S,S-C₆H₄)Fe(NO)₂]. This material is available free of charge via the Internet at <http://pubs.acs.org>. The CCDC reference numbers are 235829 and 235830.

IC049105J